Since January 2020 Elsevier has created a COVID-19 resource centre with free information in English and Mandarin on the novel coronavirus COVID-19. The COVID-19 resource centre is hosted on Elsevier Connect, the company's public news and information website.

Veterinary Microbiology 182 (2016) 57–63

Contents lists available at ScienceDirect

Veterinary Microbiology

journal homepage: www.elsevier.com/locate/vetmic

Short communication

Porcine deltacoronavirus induces apoptosis in swine testicular and LLC porcine kidney cell lines *in vitro* but not in infected intestinal enterocytes *in vivo*

Kwonil Jung*, Hui Hu, Linda J. Saif*

Food Animal Health Research Program, Ohio Agricultural Research and Development Center, College of Food, Agricultural, and Environmental Sciences, Department of Veterinary Preventive Medicine, The Ohio State University, Wooster, Ohio, USA

ARTICLE INFO

Article history:
Received 27 July 2015
Received in revised form 22 October 2015
Accepted 23 October 2015

Keywords:
Coronavirus
Porcine deltacoronavirus
Cell death
Necrosis
Apoptosis
Virus
Pig

ABSTRACT

We compared the mechanisms of porcine delatacoronavirus (PDCoV) induced death of infected enterocytes *in vivo* and infected LLC porcine kidney (LLC-PK) and swine testicular (ST) cells *in vitro*. We conducted histologic analysis and immunofluorescence (IF) staining for the detection of PDCoV antigens, and TUNEL assay in singly or serially cut tissue sections from the small and large intestines of four, 11- to 14-day-old gnotobiotic pigs, inoculated orally with 8.8–11.0 $\log_{10}$ genomic equivalents (GE) of US PDCoV strains OH-FD22 or OH-FD100 ($n = 3$), or mock ($n = 1$). Similar comparative assays were done on LLC-PK and ST cells inoculated with the cell-adapted PDCoV strain OH-FD22-P44 (passage 44) in cell culture medium with 2.5–10 μg/ml of trypsin and 1% pancreatin, respectively. At post-inoculation days 3–4, infected pigs showed severe watery diarrhea and/or vomiting and mainly, diffuse, severe atrophic enteritis, with mild to moderate cytoplasmic vacuolation of the enterocytes lining the atrophied villous epithelium. By IF, PDCoV antigens were evident in villous or crypt epithelial cells. No PDCoV antigen-positive, small and large intestinal villous or crypt epithelial cells, of which cytoplasm was also either vacuolated or morphologically normal, showed positive TUNEL staining. In contrast, by double IF and TUNEL staining, most of the TUNEL-positive signals (apoptotic nuclear fragmentation) were found in PDCoV antigen-positive LLC-PK and ST cells that also showed cytopathic effects, such as cell rounding, detachment and clumping in clusters. Secondary annexin V/propidium iodide (PI) staining revealed increased numbers of annexin V- or PI-positive LLC-PK and ST cells at 21 h after inoculation, compared to the negative controls. Thus, PDCoV does not induce apoptosis in the infected intestinal enterocytes *in vivo*, but in two infected cell lines of swine origin, LLC-PK and ST cells.

1. Introduction

Porcine deltacoronavirus (PDCoV), a member of the genus *Deltacoronavirus* in the family *Coronaviridae* of the order *Nidovirales*, causes acute diarrhea, vomiting, dehydration and mortality in nursing pigs (Jung et al., 2015; Lau et al., 2012). In the US, PDCoV was reported from clinical cases of diarrhea in young pigs in early 2014 by Wang et al. in Ohio (Wang et al., 2014), Marthaler et al. in Illinois (Marthaler et al., 2014), and Li et al. in Iowa (Li et al., 2014). The virus has spread continuously nationwide, causing deaths among nursing pigs. The disease is clinically and pathologically similar to porcine epidemic diarrhea virus (PEDV) and transmissible gastroenteritis virus (TGEV) (Jung et al., 2015), but with reportedly lower mortality rates. Experimental infection studies showed that PDCoV infects large numbers of villous epithelial cells of the small intestine at 3–4 days after oral inoculation (Chen et al., 2015; Jung et al., 2015). Infected enterocytes appeared to acutely undergo vacuolar, or hydropic, degeneration and exfoliated extensively from the villous epithelium, followed by villous atrophy (Chen et al., 2015; Jung et al., 2015). This process appeared to be associated with necrosis of infected cells. However, further studies are needed to verify whether PDCoV-infected enterocytes *in vivo* undergo necrosis or apoptosis.

PDCoV strain OH-FD22 has been successfully isolated and propagated in two epithelial cell lines of swine origin, LLC porcine kidney (LLC-PK) and swine testicular (ST) cells (Hu et al., 2015). The optimal cell culture conditions to isolate and propagate PDCoV on

* Corresponding authors at: Food Animal Health Research Program, Ohio Agricultural Research and Development Center, College of Food, Agricultural, and Environmental Sciences, Department of Veterinary Preventive Medicine, The Ohio State University, 1680 Madison Ave., Wooster, Ohio 44691, USA. Fax: +1 330 263 3677.
E-mail addresses: jung.221@osu.edu (K. Jung), saif.2@osu.edu (L.J. Saif).

http://dx.doi.org/10.1016/j.vetmic.2015.10.022
0378-1135/

LLC-PK and ST cells required supplementation of 10 μg/ml of trypsin and 1% pancreatin in cell culture maintenance medium for LLC-PK and ST cells, respectively (Hu et al., 2015). The morphological changes in PDCoV-infected LLC-PK and ST cells were similar and included enlarged, rounded, and densely granular cells that occurred singly or in clusters and then, cell shrinkage and detachment that resembled the process of apoptotic cell death (Hu et al., 2015); however, further studies are also required to clarify the mechanisms of cell death. Therefore, our study aimed to define by which cell death mechanism, necrosis or apoptosis, PDCoV causes deaths of infected enterocytes *in vivo* and infected LLC-PK or ST cells *in vitro*.

2. Materials and methods

2.1. Tissue samples

All tissue samples tested were formalin-fixed, paraffin-embedded tissues acquired from four, 11- to 14-day-old gnotobiotic (Gn) pigs, inoculated orally with 8.8 $\log_{10}$ genomic equivalents (GE) of US PDCoV strain OH-FD22 (pig 1), 11.0 $\log_{10}$ GE of OH-FD100 (pigs 2 and 3), or mock as a negative control (pig 4; 16 days of age at euthanasia). The clinical disease, fecal virus shedding, and general histopathology were reported in a previous study (Jung et al., 2015). Pigs were euthanized for pathologic examination at post-inoculation days (PIDs) 3–4.

2.2. Virus

The PDCoV OH-FD22-P44 virus was serially passaged in LLC-PK (ATCC CL-101) and ST (ATCC CRL1746) cells for a total of 44 passages and used in this study (Hu et al., 2015). The viral RNA titer of the OH-FD22-P44 used in this study was 9.9 $\log_{10}$ GE/ml, and the infectious titer was 9.7 $\log_{10}$ plaque forming units/ml. When a multiplicity of infection (MOI) of 0.1 was used for viral inoculation in LLC-PK and ST cells, a diffuse (up to 100%) cell clumping and moderate cell detachment as cytopathic effects (CPE) was generally observed in LLC-PK cells (treated with 2.5–10 μg/ml of trypsin) and ST cells (treated with 1% pancreatin) at PID 1. On the other hand, when a MOI of 0.01 was used for viral inoculation in LLC-PK and ST cells, only a 2–5% CPE was observed at PID 1 but a sudden, complete cell detachment was observed at PID 1.5–2 in LLC-PK cells (treated with 2.5–10 μg/ml of trypsin) and ST cells (treated with 1% pancreatin). Therefore, a MOI of 0.1 was used for viral inoculation in LLC-PK and ST cells for an adequate detection of apoptotic cell death as tested at PID 1 and earlier time-points. Compared with the original OH-FD22 strain, OH-FD22-P11 and -P20, passaged in both ST and LLC-PK cells, each had five nucleotide changes in the S genes (Hu et al., 2015). In both cell culture lines, the mutations observed at P11 were sustained through P40, with 100% nucleotide identity in P11, P20, and P40 (Hu et al., 2015, unpublished data). The pathogenicity of the OH-FD22-P40 in inoculated Gn pigs also appeared to be similar to that of the original field OH-FD22 virus (Hu et al., 2015, unpublished data).

2.3. Infection of PDCoV in LLC-PK and ST cells

The cell culture conditions used to infect LLC-PK cells with OH-FD22-P44 virus were as follows: washing of cells with maintenance medium [minimum essential medium (MEM) (Gibco, USA) supplemented with 1% antibiotic-antimycotic (Gibco), 1% nonessential amino acids (Gibco), and 1% HEPES (Gibco) with 2.5–10 μg/ml of trypsin (Gibco)] (MMT) 2 times, virus incubation for an hour, and then washing (with MMT) and the addition of MMT (Hu et al., 2015). The cell culture conditions used to infect ST cells were as follows: washing in maintenance medium [advanced MEM (Gibco) supplemented with 1% antibiotic-antimycotic and 1% HEPES] 2 times, incubation of virus for 1 h, and then washing of monolayers and the addition of maintenance medium with 1% pancreatin (Sigma, USA) (Hu et al., 2015). CPE, characterized by enlarged, rounded, and densely granular cells that occurred in clusters and eventual cell detachment (Hu et al., 2015), was monitored frequently in inoculated LLC-PK and ST cells. PDCoV-inoculated ST cells and LLC-PK cells at PID 1 when CPE was pronounced, but before cell detachment was complete, were fixed with 100% ethanol at 4 °C overnight for TUNEL staining. The adherent cells were also stained with green-fluorescent annexin V (Roche Applied Science, Mannheim, Germany), red-fluorescent propidium iodide (PI) (Roche Applied Science), and blue-fluorescent 4′, 6-diamidino-2-phenylindole dihydrochloride (DAPI) (Invitrogen, Carlsbad, CA) at 12 h after inoculation when no CPE was observed, and at a later time-point, *i.e.*, at 21 h after inoculation when an extensive, diffuse cell clumping (but no or slight cell detachment) was detected.

2.4. Immunofluorescence staining for the detection of PDCoV antigen in tissues or ST and LLC-PK cells

The formalin-fixed, paraffin-embedded tissues or PDCoV-infected cells were prepared and tested by immunofluorescence (IF) staining for the detection of PDCoV antigens, using hyperimmune Gn pig antiserum against OH-FD22, as described previously (Hu et al., 2015; Jung et al., 2015). Tissues from control pig 4 or trypsin (10 μg/ml) alone-treated LLC-PK and 1% pancreatin alone-treated ST cells were tested as negative controls for IF staining as well as TUNEL assay below.

2.5. Terminal deoxynucleotidyl transferase-mediated dUTP nick end labelling (TUNEL) assay in intestinal tissues or ST and LLC-PK cells

Paraffin-embedded intestinal tissues or IF-stained LLC-PK or ST cells were prepared as described above and evaluated by a TUNEL assay kit (Roche Applied Science, Mannheim, Germany) for apoptosis according to the manufacturer's instructions and as described previously (Jung et al., 2009; Sanad et al., 2015). Three serial intestinal tissue sections cut in 3-μm sections were also tested by H&E, IF staining for the detection of PDCoV antigens, and TUNEL assay, respectively. The formalin-fixed, paraffin-embedded placentomal tissue of a healthy pregnant ewe that showed a strong positive TUNEL staining (Sanad et al., 2015), was used as a positive control of *in situ* TUNEL assay. The IF-stained LLC-PK or ST cells were double-stained by TUNEL assay.

2.6. Annexin V/propidium iodide staining in ST and LLC-PK cells

In addition to TUNEL assay to detect the apoptosis-specific physiological change, nuclear fragmentation, LLC-PK or ST cells were also prepared as described above and evaluated by a annexin V/propidium iodide staining kit (Roche Applied Science) for identification of one of early apoptosis-related physiological changes, cell membrane alteration, according to the manufacturer's instructions.

3. Results

3.1. Clinical observations and histopathology of PDCoV OH-FD22 or OH-FD100-inoculated gnotobiotic piglets

All inoculated pigs at PIDs 3–4 exhibited acute, severe watery diarrhea and/or vomiting, followed by mild lethargy and dehydration. By macroscopic examination, all inoculated Gn pigs tested at PIDs 3–4 exhibited extensive thin and transparent intestinal walls

and accumulation of large amounts of yellowish fluid in the small and large intestinal lumen (Jung et al., 2015). The other internal organs appeared normal.

In general, histologic lesions were limited to the mucosal villous areas, but not crypts, of the small and large intestines, but mainly, the jejunum and ileum. Jejunal and ileal tissue sections from OH-FD22-inoculated pig 1 tested at PID 3 showed diffuse, moderate to severe villous atrophy, with frequent fusion of adjoining atrophied villi. In enteroctyes lining the epithelium of atrophied jejunal and ileal villi, there was a diffuse, moderate to severe cytoplasmic vacuolation (Fig. 1A), with up to 100% of the epithelium of moderately atrophied villi affected, as examined in 2 of 6 jejunal tissue sections. Vacuolated small intestinal enterocytes frequently contained pyknotic or hypochromic peripheral nuclei with condensed peripheral nuclear chromatin (Fig. 1A). Nuclei in non-vacuolated enterocytes lining the lower half to 100% of the epithelium of atrophied villi appeared to be arranged less basally and linearly and to be disorganized.

OH-FD100-inoculated pig 2 tested at PID 4 had diffuse, severe villous atrophy in the jejunum and ileum, with frequent fusion of atrophied villi and diffuse, mild cytoplasmic vacuolation of enterocytes, mostly located at the tips of the villi. Similarly, OH-FD100-inoculated pig 3 examined at PID 3 showed diffuse, moderate to severe villous atrophy in the jejunum and ileum, with diffuse, mild to moderate cytoplasmic vacuolation of villous epithelial cells. Similar to pig 1, nuclei in non-vacuolated enterocytes lining the lower half to 100% of the epithelium of atrophied villi appeared to be disorganized.

The other common histologic change of pigs 1–3 was a diffuse, mild to moderate vacuolation of superficial cecal/colonic epithelial cells. There was no accumulation of necrotic cells, cellular debris, or exfoliated cells from the villous epithelium in the intestinal lumina of inoculated pigs 1–3 at the test time-points. No villous atrophy or histologic lesions were evident in the remainder of the small intestine, duodenum, and other major organs of the inoculated pigs and negative control.

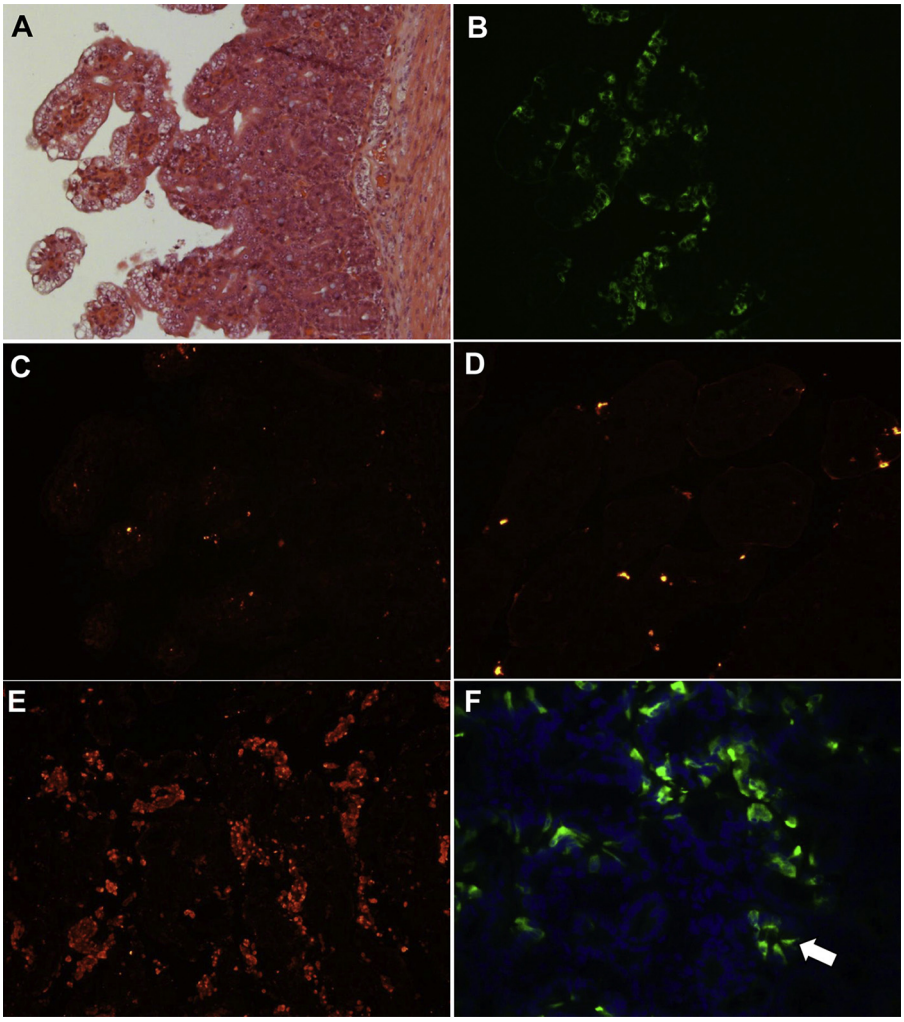

Fig. 1. Histopathology, localization of porcine deltacoronavirus (PDCoV) antigens by immunofluorescence (IF) staining, and apoptotic cells by an *in situ* TUNEL assay in the small intestine of gnotobiotic pigs inoculated with US PDCoV strain OH-FD22 or OH-FD100. (A) Hematoxylin and eosin-stained jejunum of inoculated pig 1 at post-inoculation day (PID) 3, showing acute diffuse, severe atrophic enteritis, with diffuse, moderate vacuolation of enterocytes lining the epithelium of atrophied villi. (B) IF staining of a serial section of the jejunum of inoculated pig 1 at PID 3 (Panel A), showing that the epithelial cells lining atrophied villi are positive for PDCoV antigen. (C) *In situ* TUNEL staining of a serial section of the jejunum of inoculated pig 1 (Panels A and B), showing no increase of TUNEL-positive (apoptotic) cells (red staining) in the villous epithelium positive for PDCoV antigen, compared to Panel D (negative control). (D) *In situ* TUNEL staining of formalin-fixed, paraffin-embedded jejunum of non-inoculated, negative control pig 4, showing few TUNEL-positive (apoptotic) cells (red staining) in the intestinal villous epithelium. (E) *In situ* TUNEL staining of formalin-fixed, paraffin-embedded placentome of a healthy pregnant ewe as a positive control, showing large numbers of *in situ* TUNEL-positive (apoptotic) cells (red staining) among the placental villi. (F) IF staining of jejunum of inoculated pig 2 at PID 4, showing that a few crypt epithelial cells are positive for PDCoV antigen (arrow). Nuclei were stained with blue-fluorescent 4′, 6-diamidino-2-phenylindole dihydrochloride. Original magnification, all ×200. TUNEL, terminal deoxynucleotidyl transferase-mediated dUTP nick end labelling. (For interpretation of the references to color in this figure legend, the reader is referred to the web version of this article.)

3.2. IF staining for the detection of PDCoV antigen and TUNEL assay in tissues

As determined in formalin-fixed, paraffin-embedded tissues, IF-stained cells were observed mainly in the atrophied villous epithelium of the small intestine, including the proximal jejunum to ileum, and occasionally, duodenum and cecum/colon of pigs 1–3 (Fig. 1B), as reported previously (Chen et al., 2015; Jung et al., 2015). As determined by H&E and IF staining in serial tissue sections, IF was found in large numbers of cells undergoing vacuolar degeneration as well as morphologically normal enterocytes lining the atrophied villi (Fig. 1A and B). IF was confined to the cytoplasm of the villous epithelial cells (Fig. 1B). Occasionally, however, a few small intestinal crypt epithelial cells were also positive for PDCoV antigen (Fig. 1F). No other internal organs of infected pigs showed PDCoV antigen-positive staining, as reported previously (Chen et al., 2015; Jung et al., 2015). IF-stained cells were not detected in the negative control pig.

By *in situ* TUNEL assay in singly or serially cut tissue sections from the small and large intestines of pigs 1–3, no *in situ* TUNEL-positive cells were found in the PDCoV antigen-positive intestinal villous or crypt epithelium (Fig. 1B and C). Only a few *in situ* TUNEL-positive cells were occasionally detected in the lamina propria of intestinal villi or villous epithelium of the infected pigs (Fig. 1C) and negative control (Fig. 1D), indicating that a few immune cells or mature enterocytes underwent apoptosis as a normal turnover process as tested. The placentomal tissue of a healthy pregnant ewe (Sanad et al., 2015), used as a positive control of *in situ* TUNEL assay, showed large numbers of *in situ* TUNEL-positive cells (Fig. 1E). Most of the TUNEL-positive cells appeared to be trophoblasts exfoliated from placental villi, indicating continuous refreshment of trophoblasts essential for maintaining a health placenta. As confirmed by histologic analysis, IF, and *in situ* TUNEL assay in serial intestinal tissue sections, no PDCoV-infected (PDCoV antigen-positive, vacuolated or morphologically normal), small and large intestinal villous or crypt epithelial cells showed TUNEL staining.

3.3. IF staining for the detection of PDCoV antigen and TUNEL assay in LLC-PK and ST cells

CPE in inoculated LLC-PK and ST cells was usually observed by PID 1. The morphological changes in the OH-FD22-P44-infected LLC-PK and ST cells at PID 1 were characterized by enlarged, rounded, and densely granular cells that occurred in clusters (Fig. 2A), as reported previously (Hu et al., 2015). The infected cells appeared to be shrunken and eventually detached from the monolayer (Fig. 2A) (Hu et al., 2015). The single or clustered cells that showed evident CPE, were positive for PDCoV antigen by IF staining (Figs. 2 A and 3 A). Occasionally, small numbers of cells were weakly positive for PDCoV antigen at PID 1, but with no evidence of CPE (Fig. 4A and B).

By double IF and TUNEL staining, most of the TUNEL-positive signals were found in the PDCoV antigen-positive LLC-PK and ST cells that also showed CPE, such as cell rounding and clumping in clusters (Figs. 2 A–C and 3 A–C). TUNEL-positive signals were characterized by clusters of multiple small, round, dense, fragmented, red staining (Figs. 2 B and 3 B), which appeared to be fragmentation of the nucleus into multiple nuclear membrane-bound chromatin (apoptotic) bodies. Frequently, PDCoV antigen-positive, but CPE-negative cells did not show TUNEL-positive staining (Fig. 4A–C), indicating that the nuclei of these infected cells did not undergo fragmentation when tested. The trypsin- or pancreatin alone groups showed no CPE, IF- or TUNEL-positive staining (Figs. 2 D and 3 D).

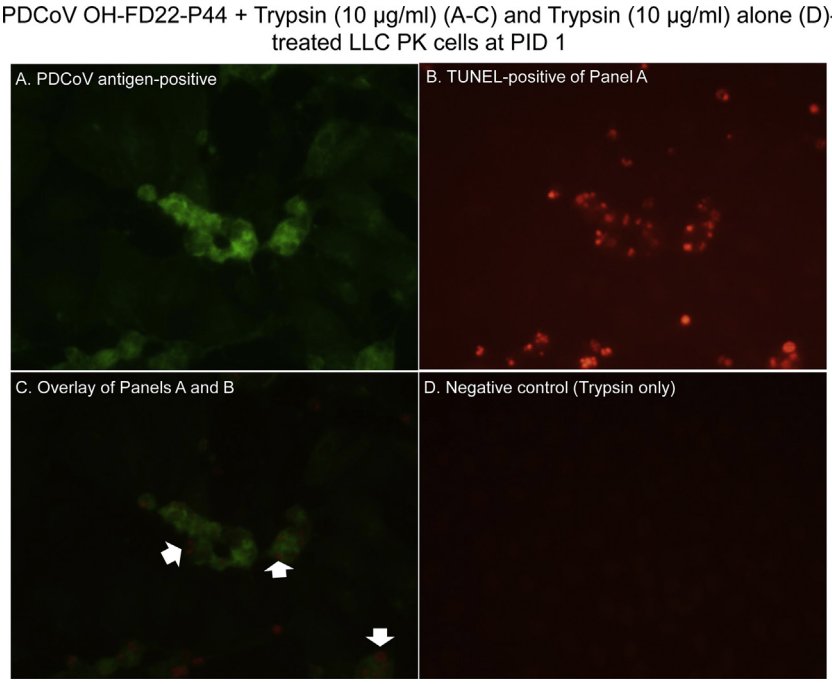

Fig. 2. Localization of porcine deltacoronavirus (PDCoV) antigens by immunofluorescence (IF) staining and apoptotic cells by a TUNEL assay in the LLC porcine kidney (LLC-PK) cells inoculated with the cell-adapted PDCoV strain OH-FD22 (virus passage number, 44), as supplemented with 10 µg/ml of trypsin in cell culture medium. (A) IF staining of the inoculated LLC-PK cells at PID 1, showing that the enlarged, rounded, and clustered cells are positive for PDCoV antigen (green staining). (B) Double TUNEL staining of Panel A, showing that the cytopathic effect (CPE)- and PDCoV antigen-positive cells are TUNEL-positive (intranuclear red staining). (C) Overlay of Panels A and B, confirming that CPE- and PDCoV antigen-positive cells show TUNEL-positive signals (red staining; arrows). (D) TUNEL staining of non-inoculated, trypsin (10 µg/ml) only-treated LLC-PK cells at PID 1, showing no TUNEL-positive cells. Original magnification, all ×600. TUNEL, terminal deoxynucleotidyl transferase-mediated dUTP nick end labelling. (For interpretation of the references to color in this figure legend, the reader is referred to the web version of this article.)

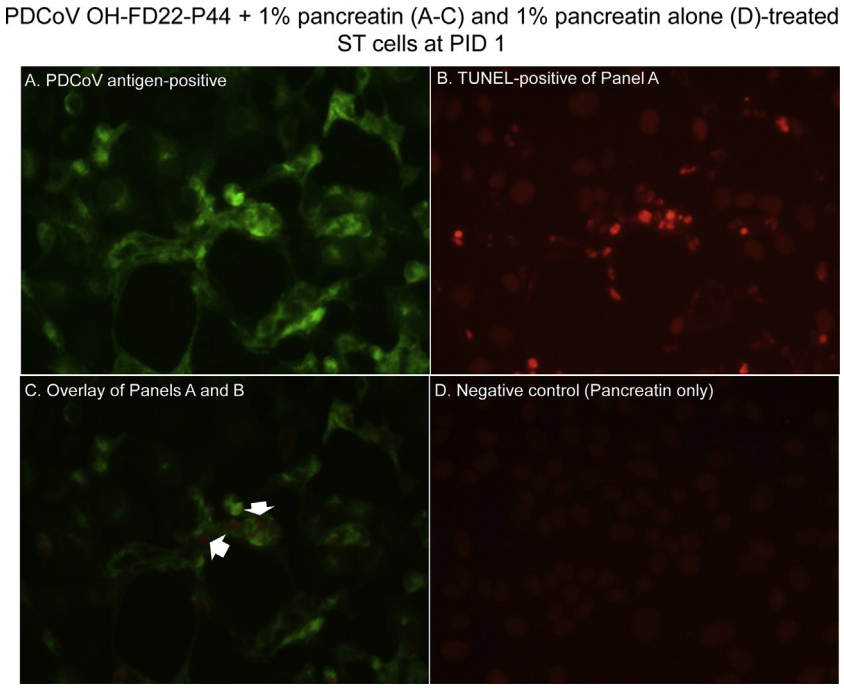

Fig. 3. Localization of porcine deltacoronavirus (PDCoV) antigens by immunofluorescence (IF) staining and apoptotic cells by a TUNEL assay in the swine testicular (ST) cells inoculated with the cell-adapted PDCoV strain OH-FD22 (virus passage number, 44), as supplemented with 1% pancreatin in cell culture medium. (A) IF staining of the inoculated ST cells at PID 1, showing that the enlarged, rounded, and clustered cells are positive for PDCoV antigen (green staining). (B) Double TUNEL staining of Panel A, showing that the cytopathic effect (CPE)- and PDCoV antigen-positive cells are TUNEL-positive (intranuclear red staining). (C) Overlay of Panels A and B, confirming that CPE- and PDCoV antigen-positive cells show TUNEL-positive signals (red staining; arrows). (D) TUNEL staining of non-inoculated, 1% pancreatin only-treated ST cells at PID 1, showing no TUNEL-positive cells. Original magnification, all ×600. TUNEL, terminal deoxynucleotidyl transferase-mediated dUTP nick end labelling. (For interpretation of the references to color in this figure legend, the reader is referred to the web version of this article.)

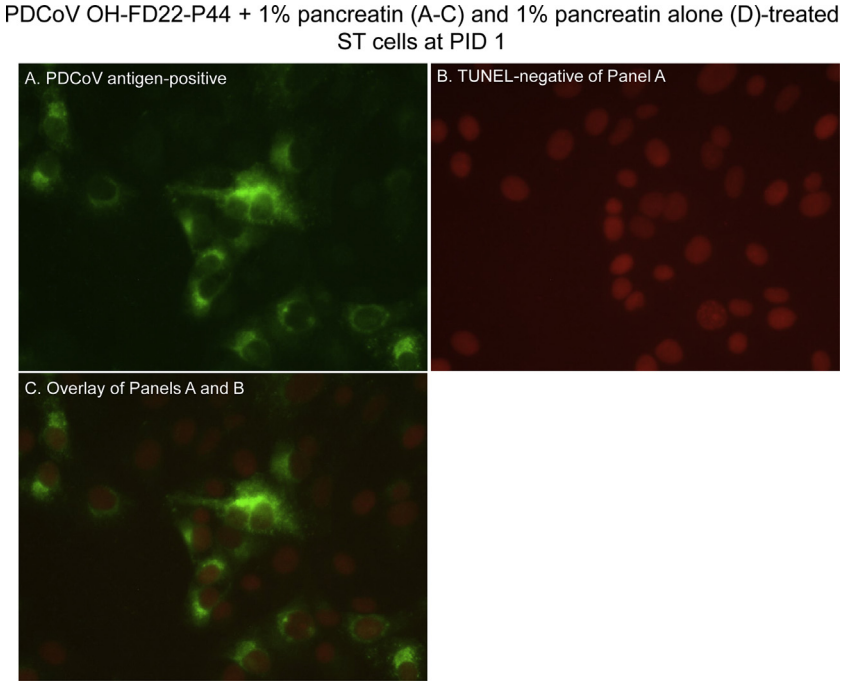

Fig. 4. Localization of porcine deltacoronavirus (PDCoV) antigens by immunofluorescence (IF) staining and apoptotic cells by a TUNEL assay in the swine testicular (ST) cells inoculated with the cell-adapted PDCoV strain OH-FD22 (virus passage number, 44), as supplemented with 1% pancreatin in cell culture medium. (A) IF staining of the inoculated ST cells at PID 1, showing that the cells positive for PDCoV antigen (green staining) exhibit no cytopathic effect (CPE). (B) Double TUNEL staining of Panel A, showing that the cells positive for PDCoV antigen but negative for CPE are TUNEL-negative. (C) Overlay of Panels A and B, confirming that the cells positive for PDCoV antigen but negative for CPE are TUNEL-negative. Original magnification, all ×600. TUNEL, terminal deoxynucleotidyl transferase-mediated dUTP nick end labelling. (For interpretation of the references to color in this figure legend, the reader is referred to the web version of this article.)

3.4. Annexin V/propidium iodide staining in LLC-PK and ST cells

At 12 h after inoculation, virus-inoculated and non-inoculated LLC-PK cells (mean 115.7 ± 10.1 cells) in the microscopic area, ×600 magnification, commonly showed a few cells (<6 cells) positive for annexin V, which were also positive for both PI and DAPI. Thus, the few annexin V+/PI+ cells observed in both treatment groups might indicate eventual death of aged cells at the time tested. At 21 h after inoculation, there were increased numbers of annexin V+ cells (mean 14.7 ± 2.1 cells), which were also positive for both PI and DAPI (Fig. 5A), regarded as representative of late-stage of apoptosis or necrosis, compared to a few (<6 cells/×600 microscopic area) annexin V+/PI+ cells in the non-inoculated LLC-PK cells at the same time tested (Fig. 5B).

On the other hand, at 12 h after inoculation, virus-inoculated and non-inoculated ST cells (mean 177.7 ± 5.1 cells) in the microscopic area, ×600 magnification, commonly showed a few cells (<3 cells) positive for annexin V, which were also positive for both PI and DAPI. Thus, the few annexin V+/PI+ cells observed in both treatment groups might indicate eventual death of aged cells at the time tested. At 21 h after inoculation when the extent of CPE in ST cells was similar to that in LLC-PK cells, there were slightly increased numbers of annexin V+/PI- cells (mean 4.8 ± 2.5 cells) (Fig. 5C), regarded as representative of early-stage of apoptosis, and annexin V−/PI+ (mean 6.8 ± 2.4 cells) (Fig. 5C), regarded as representative of late-stage of apoptosis or necrosis, compared to a few annexin V+/PI+ cells (<3 cells/×600 microscopic area) in the non-inoculated ST cells at the same time tested (Fig. 5D). There were also a few annexin V+/PI+ cells (<2 cells/×600 microscopic area) in the inoculated ST cells at the time tested.

4. Discussion

Based on our data, vacuolar degeneration and eventual death observed in PDCoV-infected intestinal villous epithelial cells is not due to apoptosis, but possibly, necrosis as a result of the cytolytic action(s) of the virus. In general, acute vacuolation or swelling of cytoplasm characterizes cell death caused by hypoxia as a result of failure of the sodium–potasium ion pump mechanism (Jones et al., 1997). Cytolytic viruses cause necrosis of infected cells by interfering with their ability to synthesize proteins and produce energy essential for maintaining cell life and homeostasis; and mechanically damaging cellular organelles and membranes with accumulations of large amounts of viral nucleic acids and/or proteins (Jones et al., 1997). We speculate that these are possible

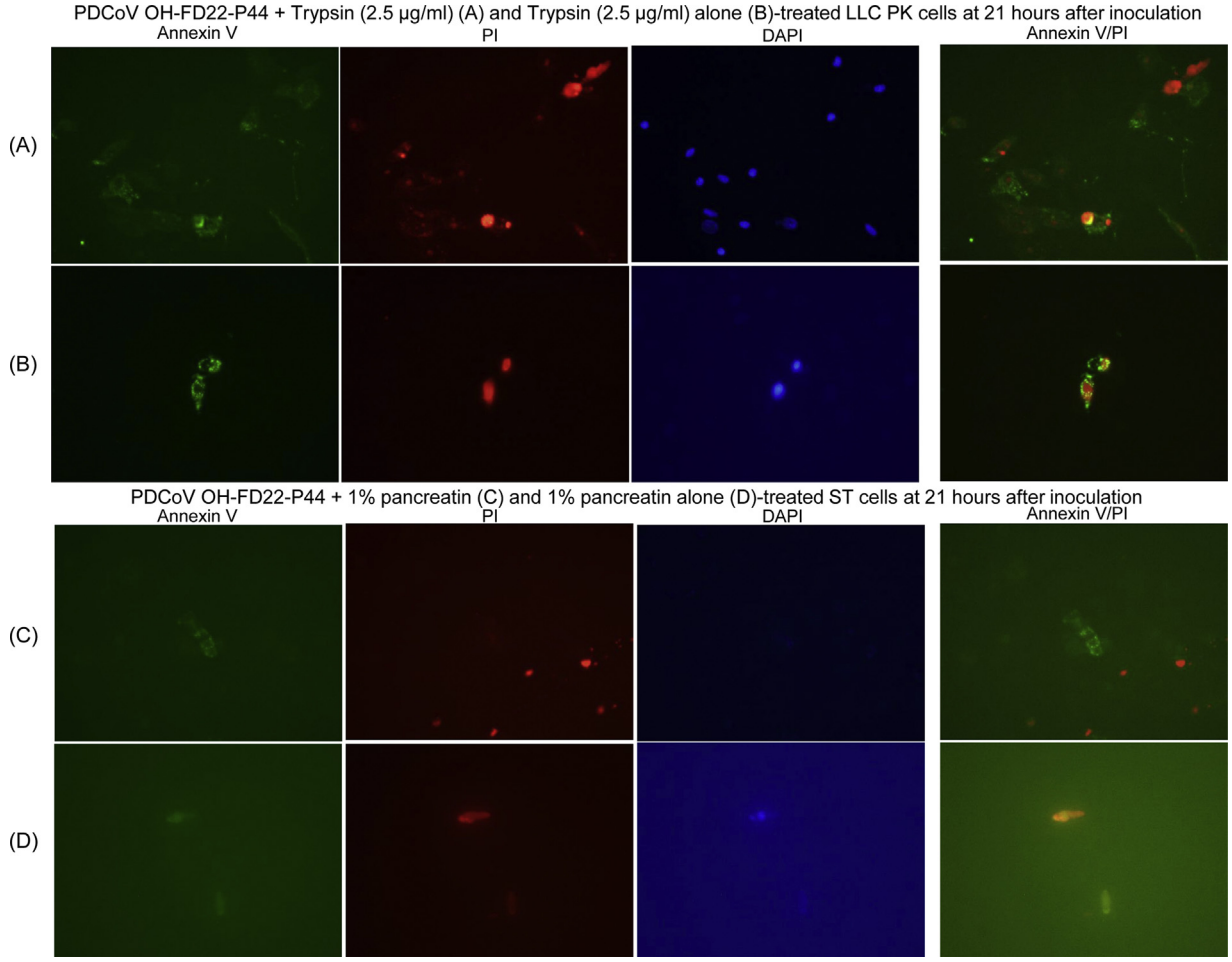

Fig. 5. Annexin V staining in the LLC porcine kidney (LLC-PK) cells (A and B) and swine testicular (ST) cells (C and D) inoculated with the cell-adapted PDCoV strain OH-FD22 (virus passage number, 44), as supplemented with 2.5 μg/ml of trypsin or 1% pancreatin in cell culture medium. (A) Green-fluorescent annexin V, red-fluorescent propidium iodide (PI), and blue-fluorescent 4′, 6-diamidino-2-phenylindole dihydrochloride (DAPI) staining of the inoculated LLC-PK cells at 21 h after inoculation, showing a small number of annexin V+/PI+/DAPI+ cells. (B) Green-fluorescent annexin V, red-fluorescent PI, and blue-fluorescent DAPI staining of non-inoculated, trypsin (2.5 μg/ml) only-treated LLC-PK cells at 21 h after inoculation, showing few annexin V+/PI+/DAPI+ cells. (C) Green-fluorescent annexin V, red-fluorescent PI, and blue-fluorescent DAPI staining of the inoculated ST cells at 21 h after inoculation, showing a small number of annexin V+/PI− or annexin V−/PI+ cells. (D) Green-fluorescent annexin V, red-fluorescent PI, and blue-fluorescent DAPI staining of non-inoculated, 1% pancreatin only-treated ST cells at 21 h after inoculation, showing few annexin V+/PI+ cells. Original magnification, all ×600. (For interpretation of the references to color in this figure legend, the reader is referred to the web version of this article.)

causes of vacuolar degeneration and death of PDCoV-infected enterocytes *in vivo*.

Apoptotic cells are pathologically characterized by nuclear and cytoplasmic shrinkage and nuclear fragmentation without significant damage of nuclear and cytoplasmic membranes. On the other hand, when necrotic cells acutely undergo swelling or vacuolation of the cytoplasm and then irreversible injury of cytoplasmic membrane, they are mostly characterized by irreversible nuclear alterations, such as pyknosis, karyorrhexis, or karyolysis, due to permanent disruption of nuclear membranes. These distinct pathological aspects may differentiate necrosis from apoptosis.

Eukaryotic cells infected by viruses mostly undergo either necrosis or apoptosis, or neither by viral inhibition of either cell death processes (Miller and Fox, 2004), depending on the viral strategy, leading to efficient viral replication and survival in infected cells. The latter example includes classical swine fever virus (CSFV) causing no death of infected SWC3+ granulocytes as the major replication site of the virus in infected pigs, but apoptosis of bystander cells, CD4+ and CD8+ T cells (Ganges et al., 2008). Viral inhibition of necrosis or apoptotic cell death of infected cells may also prolong survival of intracellular virus (Miller and Fox, 2004). In contrast to the capacity of PDCoV to induce necrosis of infected enterocytes *in vivo*, death of PDCoV-infected LLC-PK or ST cells is *via* apoptosis, directly related to viral infection and replication. In our study, TUNEL-positive signals (apoptotic nuclear fragmentation) were mostly in LLC-PK or ST cells positive for both PDCoV antigen and virus-induced CPE. Our study also identified increased numbers of inoculated LLC-PK or ST cells positive for annexin V as a marker of one of early apoptosis-related physiological changes, cell membrane alteration. Based on our annexin V/PI staining results, in LLC-PK cells at 21 h after inoculation, the cells positive for both annexin V and PI might include late-stage apoptotic cells or necrotic cells. On the other hand, in ST cells at 21 h after inoculation when the extent of CPE was similar to that in inoculated LLC-PK cells, there were both early-stage apoptotic cells and late-stage apoptotic cells or necrotic cells.

Similar to PDCoV, the other 2 swine enteric coronaviruses, PEDV and TGEV, are cytolytic in infected enterocytes *in vivo* (Jung and Saif, 2015; Kim et al., 2000) and in PEDV-infected Vero (African green monkey kidney) cell lines (Kim and Lee, 2014) and TGEV-infected ST cell lines (Eleouet et al., 1998) *in vitro*. For efficient replication and survival in each environment, PEDV and TGEV likely induce vacuolar degeneration or necrosis of infected enterocytes *in vivo* (Jung and Saif, 2015; Kim et al., 2000), whereas they also cause apoptotic cell death of infected Vero (Kim and Lee, 2014) or ST cells (Eleouet et al., 1998) *in vitro*. Based on these observations, a study of the mechanisms related to cell death caused by PEDV, TGEV, or PDCoV in *in vitro* conditions may not be applicable for the comprehensive understanding of cell death of infected enterocytes that occurs *in vivo*. Our findings indicate the necessity of an *in vitro* system to be able to better mimic *in vivo* conditions, such as intestinal enteroids or organoids (Finkbeiner et al., 2012), and also implicate the limited *in vivo* significance of the cell death studies related to *in vitro* observations.

5. Conclusion

Clarification of the forms of cell death caused by infection of viruses under *in vivo* and *in vitro* conditions is critical to explore the anti-viral pathways. Our present study revealed that PDCoV does not induce apoptosis in the infected intestinal enterocytes *in vivo*, but apoptosis is induced in two cell lines of swine origin which have been used for the isolation and propagation of PDCoV, LLC-PK and ST cells. Future studies are needed to delineate the detailed mechanisms involved in cell death of PDCoV-infected cells in the *in vivo* and *in vitro* microenvironment.

Conflict of interest

Neither of the authors of this paper has a financial or personal relationship with other people or organizations that could inappropriately influence or bias the content of the paper.

Acknowledgements

We thank Dr. Juliette Hanson, Ronna Wood, and Jeffery Ogg for assistance with animal care; Dr. Gireesh Rajashekara for providing the ovine placentomal tissue; and Zhongyan Lu for technical assistance. Salaries and research support were provided by state and federal funds appropriated to the Ohio Agricultural Research and Development Center, The Ohio State University. This work was supported by Four Star Animal Health (Saif L.J., PI) and a grant from the OARDC SEEDS, Grant # OAOH1536 (Jung K., PI).

References

Chen, Q., Gauger, P., Stafne, M., Thomas, J., Arruda, P., Burrough, E., Madson, D., Brodie, J., Magstadt, D., Derscheid, R., Welch, M., Zhang, J., 2015. Pathogenicity and pathogenesis of a United States porcine deltacoronavirus cell culture isolate in 5-day-old neonatal piglets. Virology 482, 51–59.

Eleouet, J.F., Chilmonczyk, S., Besnardeau, L., Laude, H., 1998. Transmissible gastroenteritis coronavirus induces programmed cell death in infected cells through a caspase-dependent pathway. J. Virol. 72, 4918–4924.

Finkbeiner, S.R., Zeng, X.L., Utama, B., Atmar, R.L., Shroyer, N.F., Estes, M.K., 2012. Stem cell-derived human intestinal organoids as an infection model for rotaviruses. mBio 3, 00159–100112.

Ganges, L., Nunez, J.I., Sobrino, F., Borrego, B., Fernandez-Borges, N., Frias-Lepoureau, M.T., Rodriguez, F., 2008. Recent advances in the development of recombinant vaccines against classical swine fever virus: cellular responses also play a role in protection. Vet. J. 177, 169–177.

Hu, H., Jung, K., Vlasova, A.N., Chepngeno, J., Lu, Z., Wang, Q., Saif, L.J., 2015. Isolation and characterization of porcine deltacoronavirus from pigs with diarrhea in the United States. J. Clin. Microbiol. 53, 1537–1548.

Jones, T.C., Hunt, R.D., King, N.W., 1997. Veterinary Pathology, 6th ed. Lippincott Williams & Wilkins, pp. 1–24.

Jung, K., Hu, H., Eyerly, B., Lu, Z., Chepngeno, J., Saif, L.J., 2015. Pathogenicity of 2 porcine deltacoronavirus strains in gnotobiotic pigs. Emerg. Infect. Dis. 21, 650–654.

Jung, K., Renukaradhya, G.J., Alekseev, K.P., Fang, Y., Tang, Y., Saif, L.J., 2009. Porcine reproductive and respiratory syndrome virus modifies innate immunity and alters disease outcome in pigs subsequently infected with porcine respiratory coronavirus: implications for respiratory viral co-infections. J. Gen. Virol. 90, 2713–2723.

Jung, K., Saif, L.J., 2015. Porcine epidemic diarrhea virus infection: etiology, epidemiology, pathogenesis and immunoprophylaxis. Vet. J. 204, 134–143.

Kim, B., Kim, O., Tai, J.H., Chae, C., 2000. Transmissible gastroenteritis virus induces apoptosis in swine testicular cell lines but not in intestinal enterocytes. J. Comp. Pathol. 123, 64–66.

Kim, Y., Lee, C., 2014. Porcine epidemic diarrhea virus induces caspase-independent apoptosis through activation of mitochondrial apoptosis-inducing factor. Virology 460–461, 180–193.

Lau, S.K., Woo, P.C., Yip, C.C., Fan, R.Y., Huang, Y., Wang, M., Guo, R., Lam, C.S., Tsang, A.K., Lai, K.K., Chan, K.H., Che, X.Y., Zheng, B.J., Yuen, K.Y., 2012. Isolation and characterization of a novel Betacoronavirus subgroup A coronavirus, rabbit coronavirus HKU14, from domestic rabbits. J. Virol. 86, 5481–5496.

Li, G., Chen, Q., Harmon, K.M., Yoon, K.J., Schwartz, K.J., Hoogland, M.J., Gauger, P.C., Main, R.G., Zhang, J., 2014. Full-length genome sequence of porcine deltacoronavirus strain USA/IA/2014/8734. Genome Announc. 2, e278–e314.

Marthaler, D., Jiang, Y., Collins, J., Rossow, K., 2014. Complete genome sequence of strain SDCV/USA/Illinois121/2014, a porcine deltacoronavirus from the United States. Genome Announc. 2, e218–e314.

Miller, L.C., Fox, J.M., 2004. Apoptosis and porcine reproductive and respiratory syndrome virus. Vet. Immunol. Immunopathol. 102, 131–142.

Sanad, Y.M., Jung, K., Kashoma, I., Zhang, X., Kassem, I.I., Saif, Y.M., Rajashekara, G., 2015. Insights into potential pathogenesis mechanisms associated with Campylobacter jejuni-induced abortion in ewes. BMC Vet. Res. 10, 274.

Wang, L., Byrum, B., Zhang, Y., 2014. Detection and genetic characterization of deltacoronavirus in pigs, Ohio, USA, 2014. Emerg. Infect. Dis. 20, 1227–1230.